ChemComm

COMMUNICATION

View Article Online
View Journal | View Issue

Cite this: *Chem. Commun.*, 2017, 53, 12282

Received 13th July 2017,
Accepted 16th October 2017

DOI: 10.1039/c7cc05423h

rsc.li/chemcomm

Programming membrane permeability using integrated membrane pores and blockers as molecular regulators†

Julia M. Thomas,[a] Mark S. Friddin,[a] Oscar Ces[ab] and Yuval Elani*[ab]

We report a bottom-up synthetic biology approach to engineering vesicles with programmable permeabilities. Exploiting the concentration-dependent relationship between constitutively active pores (alpha-hemolysin) and blockers allows blockers to behave as molecular regulators for tuning permeability, enabling us to systematically modulate cargo release kinetics without changing the lipid fabric of the system.

The use of biologically derived molecular components has proved to be a powerful strategy for the design and assembly of a rich and diverse range of lipid-bilayer encased microsystems. They enable a repertoire of biomimetic features to be incorporated into cell-like architectures[1] including motility,[2] protein synthesis,[3] and enzymatic reaction cascades,[4] in addition to mechanosensitive behaviours,[5] active molecular transport,[6] and light-activated responses.[7]

This repurposing of biological machinery to impart functionality into artificial systems is one of the core tenants of bottom-up synthetic biology, which has shown promise in developing a new generation of liposomal drug delivery systems,[8,9] vesicle-based microreactors,[4,10,11] and membrane-bound artificial cells.[3,12–15] Here, we exploit this strategy to construct Giant Unilamellar Vesicles (GUVs) with user-defined permeabilities. Crucially our approach does not rely upon chemical modification or breakdown of the lipid chassis and instead exploits the interactions between embedded membrane protein pores and chemical blockers.

Fundamental to successful applications for these technologies is the ability to precisely control the exchange of materials between individual compartments and the external medium. This is critical for controlling drug release rates, modulating reaction kinetics, mediating communication between artificial cells and neighbouring biological cells,[13] and regulating the interchange of nutrients and waste products.[3] To date, this has been achieved by triggering the free-diffusion of materials through protein channels inserted into the membrane or by releasing the entire contents of the compartment by lysis. Alternative approaches involve generating defects in the membrane fabric, *e.g.* through UV irradiation,[16] photocleavage,[17–19] photoisomerisation,[20] molecular absorbers,[21,22] by taking the membrane through a phase transition,[23,24] and application of shear forces,[25] electric fields,[11,26] osmotic gradients and changes in pH.[27]

These approaches rely on the application of external forces and the extent of permeability cannot be controlled systematically. They are not only binary in nature but also offer no sustainable control over bilayer permeability, especially if the compartment is destroyed in the process. Herein we address this problem by demonstrating that membrane permeability can be finely tuned by exploiting the relationship between a constitutively active membrane pore, alpha-hemolysin (α-HL), and the reversible blocker TRIMEB (heptakis(2,3,6-tri-*O*-methyl)-β-cyclodextrin).

α-HL is a heptameric transmembrane pore from *Staphylococcus aureus* that has a water-accessible channel lumen that is 1.4 nm wide at its narrowest point through which molecules can passively diffuse.[28,29] It can thus be used as a molecular sieve: it is permeable to globular molecules up to 2000 Da in size[30] (a category which most drugs and metabolites fall under), and longer elongated polymers,[31] yet is impermeable to biological macromolecules (including DNA and proteins). This makes it suitable for use in vesicle-based enzymatic reactors and artificial cells. TRIMEB is a cyclic oligosaccharide that reversibly and non-covalently binds to the α-HL pore lumen on the *cis* side of the barrel near Met 113,[32] restricting the passage of molecules.[32,33] The extent of blockage and the proportion of time the blocker is in the bound state contributes to total leakage through the pore, a process previously quantified using optical ion flux.[34] Due to the larger size of the blocker compared to the pore, it is unlikely that TRIMEB itself can fully translocate through α-HL.

[a] *Department of Chemistry, Imperial College London, Exhibition Road, London, SW7 2AZ, UK. E-mail: yuval.elani10@imperial.ac.uk*
[b] *Institute of Chemical Biology, Imperial College London, Exhibition Road, London, SW7 2AZ, UK*

† Electronic supplementary information (ESI) available: Experimental details. See DOI: 10.1039/c7cc05423h

Supported by single-channel electrical measurements in droplet interface bilayers (DIBs), we show that this relationship can be leveraged to carefully control the rate of release of a fluorescent dye contained within α-HL functionalised GUVs. We achieve this by regulating the concentration of TRIMEB co-encapsulated inside the GUVs, which acts as an adapter molecule, enabling the permeability of the GUV to be precisely pre-determined (Fig. 1A). Our approach does not rely upon chemical modification to the vesicles or the application of externally applied forces, and does not lead to the destruction of the membrane chassis.

1-Palmitoyl-2-oleoyl-*sn-glycero*-3-phosphocholine (POPC) GUVs in TRIS buffer (25 mM Tris–HCl; 500 mM KCl; pH 8.0) were prepared by the emulsion phase transfer technique.[35] The effect of blocker concentration was studied by encapsulating 1 mM calcein with TRIMEB concentrations ranging from 1–50 mM. An inverted fluorescence microscope (FITC filter; 200 ms exposure) was used to quantify dye leakage, with vesicle contours and mean fluorescence extracted using a thresholding function of an image analysis software (Image J). Data from a minimum of 10 GUVs were taken for each experimental condition (full experimental details are available in the ESI†). α-HL was added to the external solution as water soluble monomers (final concentration 50 ng μL^{-1}) which proceeded to bind to the membrane and assemble into the pore complex.

After a variable lag phase of between 5 and 60 minutes (Fig. 1B and C), GUV fluorescence was found to decay exponentially following the addition of the protein. We attribute this lag to the time taken for α-HL monomers to bind to the membrane and to oligomerize into a functional pore. Depending on blocker concentration, the GUV interior was indistinguishable from background after 5–80 minutes. The contrast of the GUV under phase contrast microscopy also faded over time as the composition of the interior approached that of the exterior (as observed elsewhere).[36] The smaller the concentration of blocker, the quicker the fluorescence decay (Fig. 1D).

The permeability of our system (P_{eff}) can be defined by the equation below:

$$\frac{dN_p}{dt} = P_{eff}\left(\frac{N_p}{V} - c_{p0}\right) \quad (1)$$

Here, N_p is the number of encapsulated fluorescent particles, V is vesicle volume, and c_{p0} is the concentration of calcein outside the vesicle. As external calcein is removed during GUV preparation, and as the volume of the GUV is negligible compared to that of the external solution we can assume that $c_{p0} = 0$ at all times.

Only GUVs where $r > 5$ μm were analysed as these could easily be resolved using our setup. By fitting total GUV fluorescence per unit volume (which is proportional to dye concentration)[37] to the equation above we extract P_{eff} for GUVs containing embedded pores and variable amounts of blocker (Fig. 2). We note that in this case, it is not the intrinsic membrane permeability that is being measured, but the permeability of the entire vesicle/α-HL/TRIMEB assembly, eliminating the dependence on membrane area.

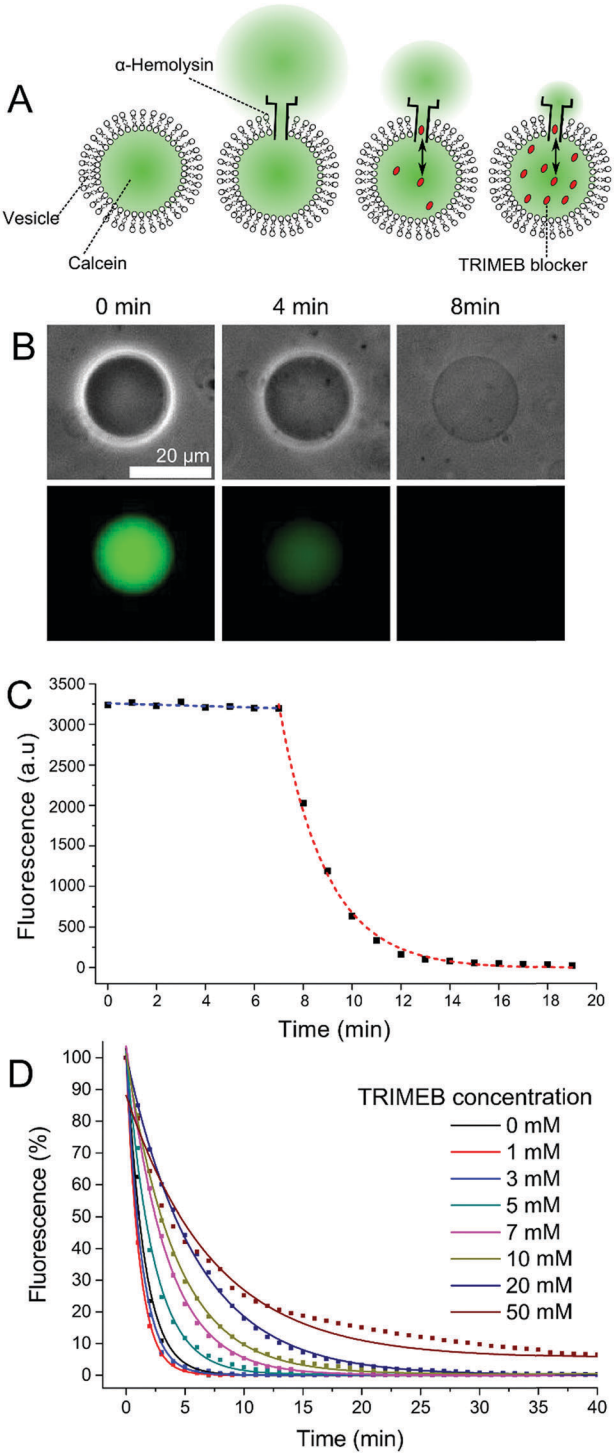

Fig. 1 Vesicle permeability fluorescence assay. (A) Schematic of the vesicle/α-HL/TRIMEB system. The presence of blocker reduces calcein flux through the pore. (B) Phase contrast and fluorescence microscopy images after a pore insertion event. As the internal and external content of the vesicle equilibrates the contrast of the membrane contour reduces. (C) Typical trace of vesicle fluorescence over time. Following a lag phase (blue) an exponential decay is seen (red) due to the formation of a pore and efflux of calcein. (D) Average vesicle fluorescence levels over time with different TRIMEB concentrations (lag phase removed). The larger the concentration of blocker the slower the decay.

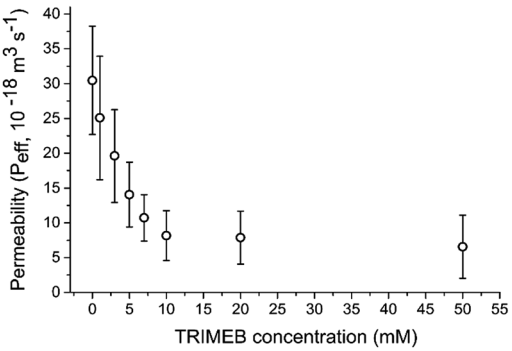

Fig. 2 Permeability values associated with the vesicle/α-HL/TRIMEB system with different concentrations of TRIMEB. Error bars = 1 standard deviation; $n > 10$.

An increase in blocker concentration led to slower dye leakage kinetics, with P_{eff} ranging from 6.6×10^{-18} m^3 s^{-1} to 30.5×10^{-18} m^3 s^{-1} in the conditions tested. Between 0 mM and 10 mM TRIMEB a linear relationship between blocker concentration and P_{eff} was observed (Pearson's r value = 0.96; $R_{adj}^2 = 0.91$), with P_{eff} decreasing 2.2×10^{-18} m^3 s^{-1} with every 1 mM increase in TRIMEB. A highly significant difference in P_{eff} was observed between eight conditions tested (ANOVA, $p < 0.0001$). These results show that blocker concentration can be used to tune membrane permeability in a quantitative manner.

As the blocker sterically prohibits passage of material through the pore, it stands to reason that changing the type of blocker will change P_{eff}. Indeed, using an analogous blocker, γ-cyclodextrin (γ-CD) with –OH as opposed to –OMe constituents on the sugar rings revealed a significantly larger P_{eff} for 20 mM of blocker (7.87×10^{-18} m^3 s^{-1} for TRIMEB and 1.58×10^{-17} m^3 s^{-1} for γ-CD; unpaired t-test, $n = 10$, $p < 0.001$). Blocker type is therefore a further parameter that can be varied in achieving defined permeabilities.

It is likely that in our system we measure single protein insertion events. We do not see a deviation from the original exponential decay curve mid-way through (which would indicate a second pore inserting). Furthermore, a probabilistic interpretation of our system makes multiple pore insertion events unlikely. Typically, only 7–10% of the GUVs leak during the course of the experiments. Assuming this is the baseline rate of single-pore insertion, and neglecting any cooperative pore insertion processes, the probability of two or more proteins inserting is between 0.5 and 1%. We also note that the permeability of the system as a whole is being measured, and it is clear that TRIMEB can be used to effectively modulate vesicle permeabilities at a given α-HL concentration, regardless of whether there is one or several pores inserting.

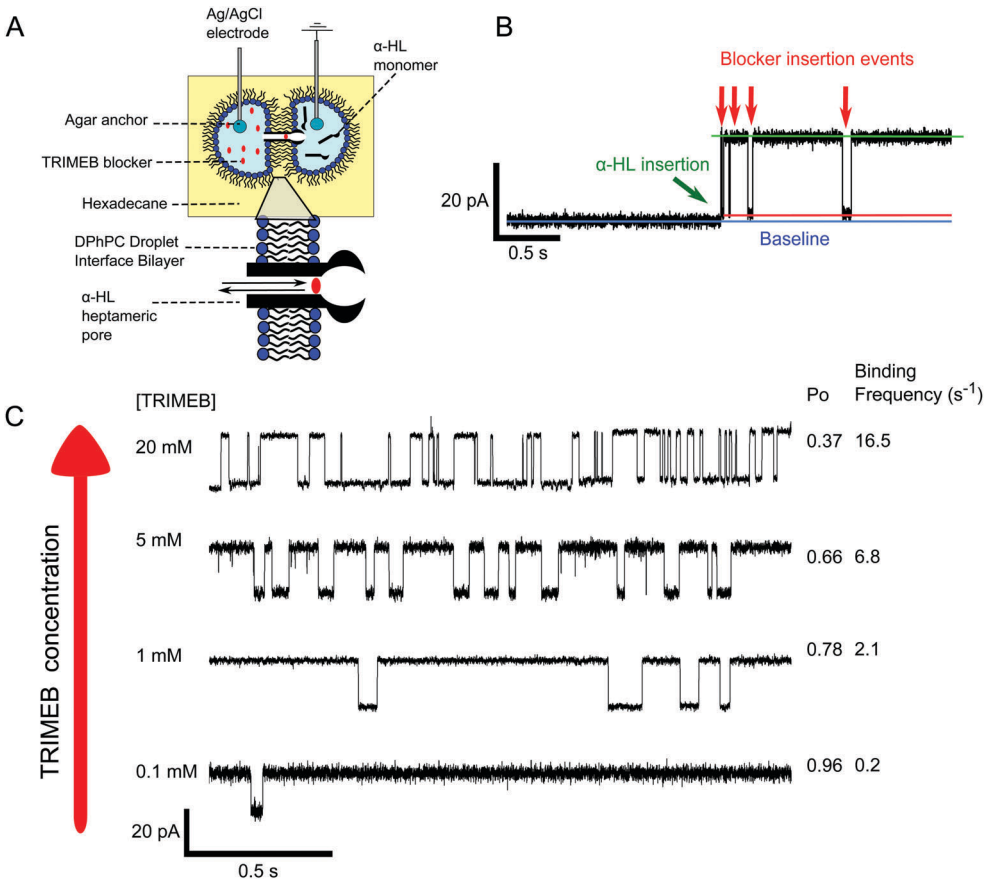

Fig. 3 Electrical interrogation of the system using DIBs. (A) Schematic of the experimental setup. (B) Trace of a typical protein insertion event followed by TRIMEB blocking events. By comparing the baseline (blue) to the fully open (green) and blocked (red) traces *ca.* 92% of the pore was estimated to be blocked. (C) Increasing TRIMEB concentration leads to more frequent blocking events and lower open probabilities.

To further probe our system at a single channel level we performed electrical measurements of droplet interface bilayers (DIBs)[38] (Fig. 3A). DIBs are planar bilayers formed when two monolayer-coated water-in-oil droplets are brought into contact. Inserting agar-coated Ag/AgCl electrodes into the droplets allows electrical interrogation. We formed DIBs from 1.5 μL water droplets containing 100 nm vesicles (formed by extrusion) made from 1,2-diphytanoyl-*sn-glycero*-3-phosphocholine (DPhPC), with one droplet containing α-HL (ground electrode), and the other TRIMEB. A holding potential of 100 mV was applied in voltage-clamp mode, and the bilayer current was measured (full experimental details available in the ESI†).

Single pore opening events were observed as *ca.* 19 pA jumps in the baseline current (in accordance with previous findings),[39] and subsequent pore blockage events by TRIMEB detected as blockades in the current (Fig. 3B). Analysis of the trace revealed that 92% of the pore was sterically blocked by the TRIMEB, which is in line with previous reports.[33] As expected, increasing TRIMEB concentration led to more frequent blocking events and lower open probabilities (P_o) (Fig. 3C), which reinforces our fluorescence microscopy results.

This system could be further optimised in future by using blockers with other channels that are not constitutively active, and by engineering α-HL mutants which have longer blocker residency times.[40] Other issues that need to be addressed for delivery applications are precise control over initiation of content release, and methods to prevent the spontaneous release of contents which limits long term storage.

In conclusion, we have developed a new method to pre-program the permeability of vesicles with fine control using a strategy that offers significant advantages over existing methods, especially as no chemical modification or vesicle lysis is required. In this approach, the structural fabric of the system remains the same with only the formulation (*i.e.* concentration of an encapsulated blocker) changing. The process of vesicle manufacture can therefore be decoupled from modulation of permeability. In principle, our method could also be applied to other channels and blockers in order to develop more elaborate synthetic biosystems with further degrees of control, and coupled, for example, to stimuli-responsive channel opening processes. This ability to finely attenuate vesicle permeability could have a significant impact on the next generation of drug delivery agents, soft-matter micro/nanoreactors, and artificial cells.

This work was supported by the EPSRC *via* grant EP/J017566/1 and by EPSRC Fellowship EP/N016998/1 awarded to YE.

Conflicts of interest

There are no conflicts to declare.

Notes and references

1 T. Trantidou, M. Friddin, Y. Elani, N. J. Brooks, R. V. Law, J. M. Seddon and O. Ces, *ACS Nano*, 2017, **11**, 6549–6565.
2 M. Guix, C. C. Mayorga-Martinez and A. Merkoçi, *Chem. Rev.*, 2014, **114**, 6285–6322.
3 V. Noireaux and A. Libchaber, *Proc. Natl. Acad. Sci. U. S. A.*, 2004, **101**, 17669–17674.
4 Y. Elani, R. V. Law and O. Ces, *Nat. Commun.*, 2014, **5**, 5305.
5 K. Charalambous, P. J. Booth, R. Woscholski, J. M. Seddon, R. H. Templer, R. V. Law, L. M. Barter and O. Ces, *J. Am. Chem. Soc.*, 2012, **134**, 5746–5749.
6 H. E. Findlay, N. J. Harris and P. J. Booth, *Sci. Rep.*, 2016, **6**, 39349.
7 V. R. Schild, M. J. Booth, S. J. Box, S. N. Olof, K. R. Mahendran and H. Bayley, *Sci. Rep.*, 2017, **7**, 46585.
8 A. Samad, Y. Sultana and M. Aqil, *Curr. Drug Delivery*, 2007, **4**, 297–305.
9 Y. Elani, R. V. Law and O. Ces, *Ther. Delivery*, 2015, **6**, 541–543.
10 P. Walde, A. Goto, P.-A. Monnard, M. Wessicken and P. L. Luisi, *J. Am. Chem. Soc.*, 1994, **116**, 7541–7547.
11 A. Fischer, A. Franco and T. Oberholzer, *ChemBioChem*, 2002, **3**, 409–417.
12 P. L. Luisi, F. Ferri and P. Stano, *Naturwissenschaften*, 2006, **93**, 1–13.
13 R. Lentini, N. l. Y. Martín, M. Forlin, L. Belmonte, J. Fontana, M. Cornella, L. Martini, S. Tamburini, W. E. Bentley and O. Jousson, *ACS Cent. Sci.*, 2017, **3**, 117–123.
14 Y. Elani, *Biochem. Soc. Trans.*, 2016, **44**, 723–730.
15 A. Salehi-Reyhani, O. Ces and Y. Elani, *Exp. Biol. Med.*, 2017, **242**, 1309–1317.
16 A. Yavlovich, A. Singh, S. Tarasov, J. Capala, R. Blumenthal and A. Puri, *J. Therm. Anal. Calorim.*, 2009, **98**, 97.
17 Y. Wan, J. K. Angleson and A. G. Kutateladze, *J. Am. Chem. Soc.*, 2002, **124**, 5610–5611.
18 N. J. Wymer, O. V. Gerasimov and D. H. Thompson, *Bioconjugate Chem.*, 1998, **9**, 305–308.
19 V. C. Anderson and D. H. Thompson, *Biochim. Biophys. Acta, Biomembr.*, 1992, **1109**, 33–42.
20 K. Kano, Y. Tanaka, T. Ogawa, M. Shimomura and T. Kunitake, *Photochem. Photobiol.*, 1981, **34**, 323–329.
21 B. Khoobehi, C. A. Char, G. A. Peyman and K. M. Schuele, *Lasers Surg. Med.*, 1990, **10**, 303–309.
22 K. A. Dendramis, P. B. Allen, P. J. Reid and D. T. Chiu, *Chem. Commun.*, 2008, 4795–4797.
23 A. Blicher, K. Wodzinska, M. Fidorra, M. Winterhalter and T. Heimburg, *Biophys. J.*, 2009, **96**, 4581–4591.
24 D. Papahadjopoulos, K. Jacobson, S. Nir and I. Isac, *Biochim. Biophys. Acta, Biomembr.*, 1973, **311**, 330–348.
25 A.-L. Bernard, M.-A. Guedeau-Boudeville, V. Marchi-Artzner, T. Gulik-Krzywicki, J.-M. di Meglio and L. Jullien, *J. Colloid Interface Sci.*, 2005, **287**, 298–306.
26 R. Dimova, N. Bezlyepkina, M. D. Jordö, R. L. Knorr, K. A. Riske, M. Staykova, P. M. Vlahovska, T. Yamamoto, P. Yang and R. Lipowsky, *Soft Matter*, 2009, **5**, 3201–3212.
27 J. Du and S. P. Armes, *J. Am. Chem. Soc.*, 2005, **127**, 12800–12801.
28 L. Song, M. R. Hobaugh, C. Shustak, S. Cheley, H. Bayley and J. E. Gouaux, *Science*, 1996, **274**, 1859–1865.
29 E. Gouaux, *J. Struct. Biol.*, 1998, **121**, 110–122.
30 R. Fussle, S. Bhakdi, A. Sziegoleit, J. Tranum-Jensen, T. Kranz and H.-J. Wellensiek, *J. Cell Biol.*, 1981, **91**, 83–94.
31 J. J. Kasianowicz, E. Brandin, D. Branton and D. W. Deamer, *Proc. Natl. Acad. Sci. U. S. A.*, 1996, **93**, 13770–13773.
32 L.-Q. Gu, O. Braha, S. Conlan, S. Cheley and H. Bayley, *Nature*, 1999, **398**, 686–690.
33 A. J. Heron, J. R. Thompson, B. Cronin, H. Bayley and M. I. Wallace, *J. Am. Chem. Soc.*, 2009, **131**, 1652–1653.
34 O. K. Castell, J. Berridge and M. I. Wallace, *Angew. Chem., Int. Ed.*, 2012, **51**, 3134–3138.
35 S. Pautot, B. J. Frisken and D. Weitz, *Langmuir*, 2003, **19**, 2870–2879.
36 P. Peterlin, G. Jaklič and T. Pisanski, *Meas. Sci. Technol.*, 2009, **20**, 055801.
37 M. Kaltenbach, S. R. Devenish and F. Hollfelder, *Lab Chip*, 2012, **12**, 4185–4192.
38 H. Bayley, B. Cronin, A. Heron, M. A. Holden, W. L. Hwang, R. Syeda, J. Thompson and M. Wallace, *Mol. BioSyst.*, 2008, **4**, 1191–1208.
39 G. Villar, A. J. Heron and H. Bayley, *Nat. Nanotechnol.*, 2011, **6**, 803–808.
40 L.-Q. Gu, S. Cheley and H. Bayley, *J. Gen. Physiol.*, 2001, **118**, 481–494.